Journal of Alloys and Compounds 509 (2011) 6061–6066

Contents lists available at ScienceDirect

Journal of Alloys and Compounds

journal homepage: www.elsevier.com/locate/jallcom

Lead titanate nanotubes synthesized via ion-exchange method: Characteristics and formation mechanism

Liang Song[a], Lixin Cao[b,a,*], Jingyu Li[b], Wei Liu[b], Fen Zhang[a], Lin Zhu[b], Ge Su[b]

[a] College of Chemistry and Chemical Engineering, Ocean University of China, Qingdao 266100, PR China
[b] Institute of Materials Science and Engineering, Ocean University of China, Qingdao 266100, PR China

ARTICLE INFO

Article history:
Received 10 November 2010
Received in revised form 3 March 2011
Accepted 3 March 2011
Available online 10 March 2011

Keywords:
Lead titanate nanotubes
Hydrothermal
Ion-exchange
Bandgap
Formation mechanism

ABSTRACT

A two-step method is presented for the synthesis of one dimensional lead titanate ($PbTi_3O_7$) nanotubes. Firstly, titanate nanotubes were prepared by an alkaline hydrothermal process with TiO_2 nanopowder as precursor, and then lead titanate nanotubes were formed through an ion-exchange reaction. We found that sodium titanate nanotubes have ion exchangeability with lead ions, while protonated titanate nanotubes have not. For the first time, we distinguished the difference between sodium titanate nanotubes and protonated titanate nanotubes in the ion-exchange process, which reveals a layer space effect of nanotubes in the ion-exchange reaction. In comparison with sodium titanate, the synthesized lead titanate nanotubes show a narrowed bandgap.

1. Introduction

Titanate nanotubes have attracted considerable attention for their potential applications in photocatalytic reaction [1–4], lithium battery [5,6], adsorption [7–9], thermoelectric property [10] and luminescence [11,12] because of their large specific surface area and unique photoelectric properties. A simple and cost effective hydrothermal method for the large scale production of titanate nanotubular material was firstly reported by Kasuga et al. [13]. Some investigations have been conducted on the phase and morphology of titanate nanotubes [14–17]. Many research groups [18–20] reported that protonated titanate nanotubes and sodium titanate nanotubes can be synthesized with and without hydrogen ion treatment. In addition, many groups have tried to analyze the synthetic mechanism, and the sheet folding mechanism of sodium titanate was often assumed [20–24].

Recently, many researchers studied the ion-exchange capacity of titanate nanotubes. Sun and Li [25] studied the ion-exchangeable behavior of titanium based nanotubes with transitional metal ions, such as Cd^{2+}, Zn^{2+}, Co^{2+}, Ni^{2+}, Cu^{2+} and Ag^{+}, and found that the absorption range of the nanotubes can be changed after ion-exchange reaction. Nanostructured silver titanate was synthesized through a silver ion-exchange treatment [26]. Ni-titanate nanotubes were synthesized from TiO_2 sol using alkali hydrothermal treatment followed by a simple ion-exchange process [27]. Jeong et al. [28] demonstrated the ion-exchange reaction between Na^{+} ions and other metal ions. Du [29] et al. found that ion-exchange feature and inner-sphere complexation of $Na_2Ti_3O_7$ nanotubes could be used for sequestration of cadmium ions. Ion-exchange feature of titanate nanotubes was used for synthesis of cation titanate nanotubes and sequestration of heavy metal ions. However, there is no discussion about the ion exchangeability of sodium titanate nanotubes and protonated titanate nanotubes, as well as their formation mechanism.

Here, we firstly introduced the ion-exchange method to synthesize lead titanate nanotubes. As far as we know, lead titanate could be used in the field of piezoelectric sensor [30,31] and electro-optic conversion [32,33]. In addition, lead titanate has shown the desired potential for use in enhanced solar energy conversion. Kim et al. [34] indicated that the hybridization of the occupied Pb *6s* and O *2p* orbital would push up the valence band, compared to undoped titanate. The ab initio DOS calculations of hybrid band demonstrated that the top of the valence band for Pb^{2+} ions modified titanate can be shifted to a higher energy level, resulting in more light absorption [35].

In this paper, we converted the nano P25 TiO_2 particles into sodium titanate nanotubes and protonated titanate nanotubes utilizing a Kasuga's method. Subsequently, a series of Pb^{2+} ion-exchange reactions were performed to investigate the exchangeable behavior of sodium titanate and protonated titanate nanotubes. The as-synthesized lead titanate nanotubes were characterized by X-ray diffraction, transmission electron microscopy

* Corresponding author. Tel.: +86 532 66781901; fax: +86 532 66781320.
E-mail address: caolixin@mail.ouc.edu.cn (L. Cao).

0925-8388/$ – see front matter © 2011 Elsevier B.V. All rights reserved.
doi:10.1016/j.jallcom.2011.03.008

Table 1
Nanotube precursors and Pb^{2+} ions sources of samples.

Sample code	Nanotube precursor	Lead ions source
TNN	TNT(Na)	$Pb(NO_3)_2$ aqueous solution
TNA	TNT(Na)	$Pb(Ac)_2$ aqueous solution
THN	TNT(H)	$Pb(NO_3)_2$ aqueous solution
THA	TNT(H)	$Pb(Ac)_2$ aqueous solution

and UV–vis diffuse reflectance spectroscopy. Furthermore, the synthetic mechanism of Pb^{2+} ion-exchangeable nanotubes was investigated.

2. Experimental

2.1. Synthesis of lead titanate nanotubes

All reagents were commercial products and used without further purification. A two-step process to synthesize lead titanate nanotubes was developed as following. Firstly, titanate nanotubes were prepared by a hydrothermal method. Briefly, 1 g TiO_2 powder (Degussa Co., P25, 70% anatase and 30% rutile) was added into a Teflon container with 52 ml of 10 M NaOH solution. The mixture was stirred for 3 h to form a uniform milk-like suspension. Then, the Teflon container was placed into a stainless steel autoclave and held at 150 °C for 24 h. After the temperature dropped to ambient temperature, the white precipitates were rinsed with deionized water and absolute ethanol, followed by centrifugation to remove excessive sodium ions and hydroxyl ions. After drying at 80 °C for 6 h, sodium titanate nanotubes, named TNT(Na), were obtained and subsequently were immersed in 250 ml 0.1 M HCl aqueous solution for 3 h to protonate the titanate nanotubes. The white precipitates were washed with deionized water and absolute ethanol, followed by drying at 80 °C for 6 h to obtain the protonated titanate nanotubes, named TNT(H). No sodium impurity was observed in the sample TNT(H) from energy dispersive X-ray spectra.

Secondly, 0.4 g TNT(Na) or TNT(H) was mixed with 0.25 mol/L Pb^{2+} ions solution at room temperature to exchange the sodium or hydrogen ions to lead ions in the interlayer of the titanate nanotubes. The molar ratio between Pb and Ti is ca. 1:1. Two kinds of lead ions containing solutions, $Pb(NO_3)_2$ and $Pb(Ac)_2$, were chosen for lead ion-exchange process. The mixtures were stirred vigorously for 1 h, followed by sonication with an ultrasonic generator for 10 min, and then violently stirred for additional 5 h. Finally, the products were collected, washed twice with deionized water and absolute ethyl alcohol, and centrifuged. The obtained precipitates were dried at 80 °C for 4 h. The ion-exchanged samples, synthesized from different precursors [TNT(Na) and TNT(H)] and lead ions containing solutions [$Pb(NO_3)_2$ and $Pb(Ac)_2$] are listed in Table 1.

2.2. Characterization

The crystalline structure of the obtained materials was examined by powder X-ray diffraction (XRD, D8 ADVANCE X-Ray diffractometer) using Cu Kα radiation under 40 kV and 40 mA. The scanned range was $2\theta = 10–70°$ with a step of 0.05° and 0.5 s/step. The tubular morphologies of lead titanate samples were investigated by a transmission electron microscope (TEM, JEM-1200 EX) using an accelerating voltage of 200 kV. The microstructure of TNT(Na) and TNT(H) nanotubes was characterized by a high resolution transmission electron microscope (HRTEM, Hitachi H-7000). The diffuse reflectance UV–vis spectra were collected on a UV-2450 spectrometer equipped with a diffuse reflectance accessory. A Zeta Potential Analyser (ZetaPlus, Brookhaven Instruments) was employed for the zeta potential measurement, where the suspension was in a plastic cuvette with path length of 10 mm. The surface charge of nanotubes was averaged from 5 runs, and each run consisted of 3 cycles.

3. Results and discussion

3.1. Structural and microscopic characteristic of ion-exchanged titanium based nanotubes

Two types of titanium based nanotubes (TNT(Na), TNT(H)) were fabricated by the hydrothermal method. Fig. 1 shows the XRD patterns of the as-prepared titanate nanotubes and ion-exchanged lead titanate nanotubes. After hydrothermal treatment and washing with water, the precursor is transformed into sodium titanate ($Na_2Ti_3O_7$), as indicated by the XRD pattern in Fig. 1a. The strong peak centered at 10.5°, which is attributed to the interlayer spacing of layer nanotubes [36], is assigned to prominent peak (0 0 1) of $Na_2Ti_3O_7$ nanotubes [37]. The obvious diffraction at $2\theta = 24.3°$, 28.2° and 48.3° are the characteristic peaks of titanate nanotubes $Na_2Ti_3O_7$ [19,38–40]. After washed by hydrochloric acid, the intensity of the peak at 28.2° decreased while the value of the peak at 24.3° increased, which indicates that the crystal structure has changed. This shift can be probably attributed to the decrease in the Na:H ratio of titanium based nanotubes, which is caused by the replacement of Na^+ with H^+ during acid washing. The monoclinic titanate $H_2Ti_3O_7$ was indicated as the phase of protonated titanate nanotubes [19,41–43].

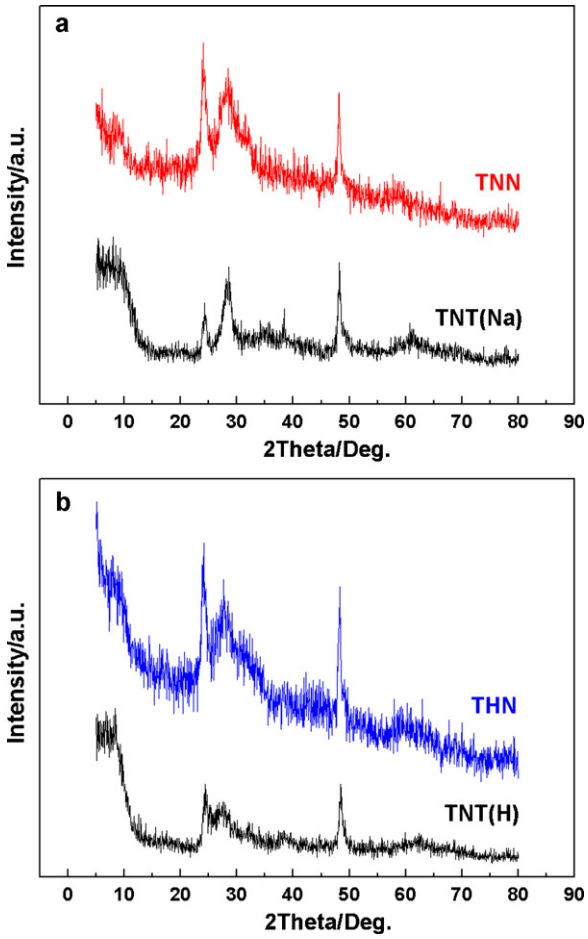

Fig. 1. XRD patterns of precursors and as-prepared ion-exchanged titanate nanotubes. (a) TNT(Na) and TNN (b) TNT(H) and THN.

After ion-exchange reaction with Pb^{2+} ions solution, the XRD pattern of THN showed the similar spectral pattern as TNT(H), as shown in Fig. 1b. However, in Fig. 1a, there is a distinct change in the relative intensity of peak 24° and 28° between the sample TNN and TNT(Na). This change indicated that the exchange between lead ions and sodium ions may have happened.

To further investigate the ion-exchange behavior between lead ions and sodium ions/hydrogen ions, the samples were calcinated at 600 °C for 3 h in air and were then studied by XRD. The XRD patterns (Fig. 2a) show that the phase of TNN samples differs from that of the precursor TNT(Na). After heat treatment, TNT(Na) was identified as $Na_{0.23}TiO_2$ (JCPDS No. 22-1404). All peaks of TNN could be indexed as $PbTi_3O_7$ phase (JCPDS No. 70-1016) and no other phase was detected, which proves the presence of Pb in the calcinated samples. This result also confirms that Na^+ ions can be exchanged by Pb^{2+} ions totally. However, TiO_2 phase was found in the heated samples of TNT(H) precursor and its ion-exchanged product THN (Fig. 2b), while no Pb-containing species were detected in the XRD pattern. In summary, these results indicate that the precursor TNT(Na) can be ion-exchanged with Pb^{2+} ions in $Pb(NO_3)_2$ aqueous solution, but the precursor TNT(H) does not possess the ion exchangeability with Pb^{2+} ions.

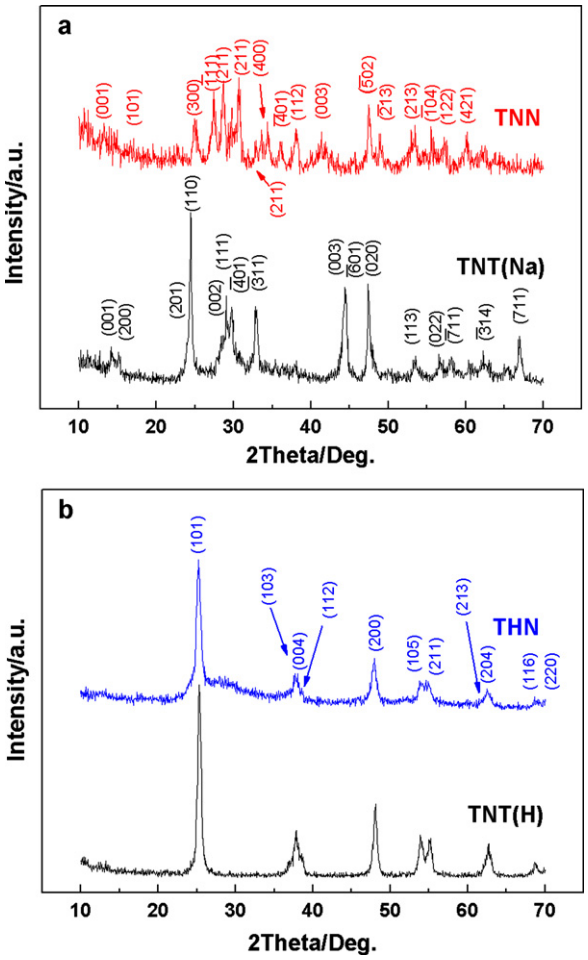

Fig. 2. XRD patterns of precursors and lead ion-exchanged nanotubes after heat treatment at 600 °C. (a) TNT(Na) and TNN and (b) TNT(H) and THN.

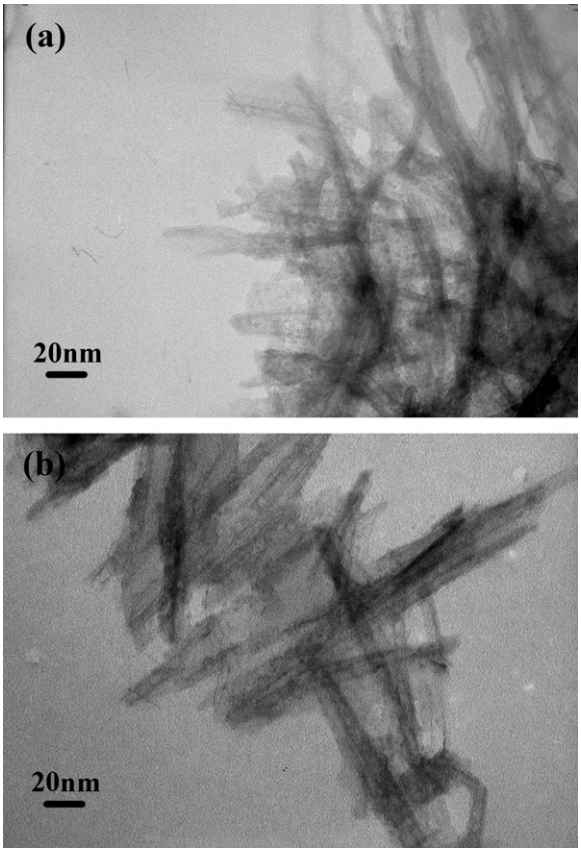

Fig. 3. TEM images of samples synthesized by different precursors. (a) TNN and (b) THN.

Fig. 3 shows the typical TEM images of lead ion-exchanged nanotubes, which demonstrates the similar microstructure of titanium based nanotubes with an outer tube diameter of 8–12 nm, inner diameter of 3–5 nm and length ranged from 50 nm to 150 nm. Photo-generated charge carries can be quickly transferred to the surface of nanotubes, because walls of these nanotubes are rather thin. The large specific surface area of nanotubes also provides more effective reaction sites for photocatalysis.

To investigate the ion-exchange behavior of nanotubes with different lead ions containing solutions, lead acetate solution was adopted as an alternative soluble salt to provide lead ions. The TNT(Na) and TNT(H) samples were reacted with lead acetate solution under the same condition as lead nitrate solution. The as-prepared samples TNA were investigated by XRD before and after heat treatment at 600 °C, and the results are illustrated in Fig. 4, which shows that the $Na_2Ti_3O_7$ nanotubes have been transformed into $PbTi_3O_7$ nanotubes after ion-exchange process with Pb^{2+} ions. However, the phase of THA sample is still anatase after heat treatment at 600 °C, similar to THN. These results indicate that the as-prepared sodium titanate nanotubes have ion exchangeability with Pb^{2+} ions, but protonated titanate nanotubes have not.

3.2. UV-vis diffuse reflectance spectra and bandgap energy determination of ion-exchanged titanium based nanotubes

Diffuse reflection spectra of different samples were investigated by the UV-2450 diffuse reflectance spectrometer, as shown in Figs. 5 and 6. As can be seen, the absorption edges of TNT(H), THN and THA samples are similar. However, the absorption curves of TNN and TNA samples show obvious red shift relative to that of TNT(Na), which indicates the energy band structure has been changed after ion-exchange process. It is well known that the conduction and valence band of TiO_2 mainly consist of Ti *3d* and O *2p*, respectively. The Pb *6s* electronic orbit does not contribute to the conduction band, but only to the valence band [34,35]. Therefore, the valence band in lead titanate nanotubes

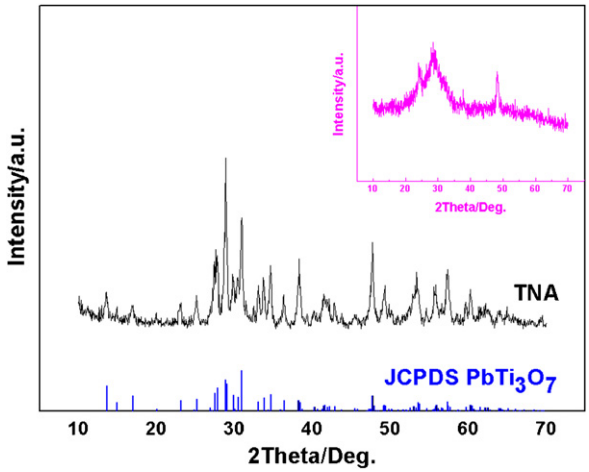

Fig. 4. XRD patterns of TNA after heat treatment at 600 °C for 3 h and the one before heat treatment (inset). The vertical bar below the patterns represents the standard diffraction data from JCPDS file for $PbTi_3O_7$ (No. 70-1016).

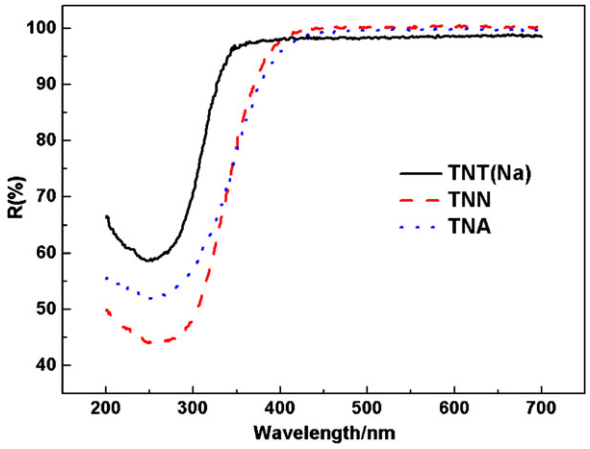

Fig. 5. Diffusion reflectance UV–vis spectra of TNT(Na), TNN and TNA.

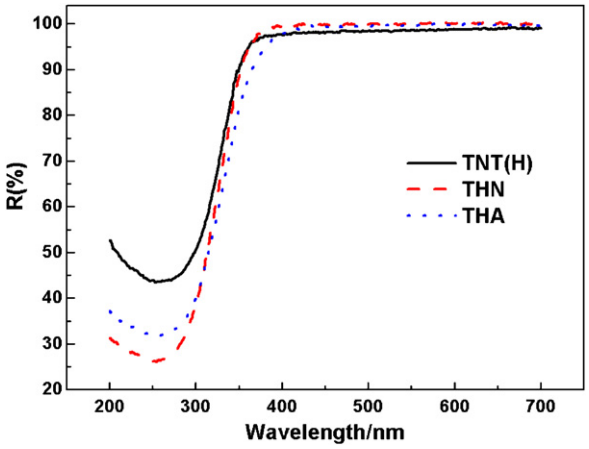

Fig. 6. Diffusion reflectance UV–vis spectra of TNT(H), THN and THA.

consists of the O *2p* and Pb *6s* hybrid orbital and the top of the valence band is shifted to the high energy side. This decrease in bandgap energy is consistent with the results in Fig. 5.

In order to quantify the effect of lead ions modification on the bandgap of titanate nanotubes, we analyzed the bandgap energy from the diffuse spectra based on Kubelka–Munk theory. According to the hypothesis of plural scattering, a diffuse reflection spectrum could be transformed into a plot of the square root of $F(R)h\upsilon$ versus the energy of irradiation. The Kubelka–Munk function [44] is shown as in Eq. (1):

$$F(R) = \frac{(1-R)^2}{2R} \tag{1}$$

Here, R is the measured reflectance ($R = R_{sample}/R_{reference}$). The use of $F(R)$ as the equivalent of absorbance relies on the assumption that the scattering coefficients were consistent throughout the compared samples [45]. From Yeong Kim's results, the optical absorption behavior of lamellar titanate is consistent with a indirect gap semiconductor [46]. So, the bandgap can be estimated form

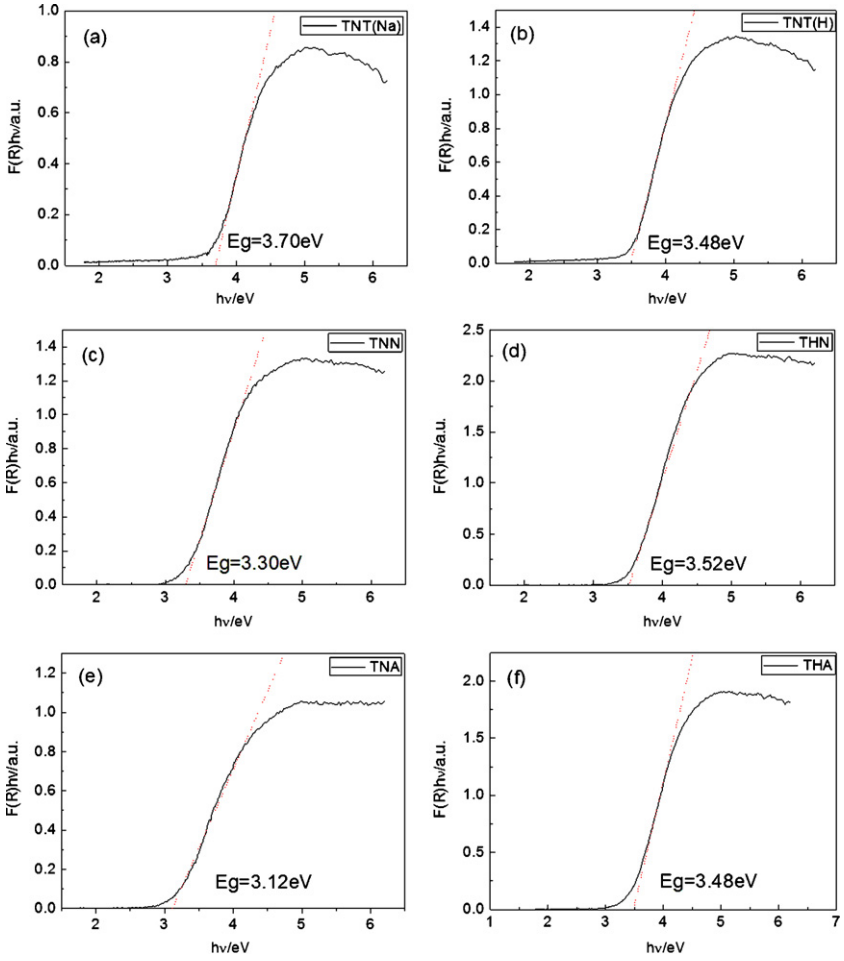

Fig. 7. The Kubelka–Munk transit of diffusion reflectance UV–vis spectra. (a) TNT(Na), (b)TNT(H), (c)TNN, (d)THN, (e)TNA, and (f)THA. E_g stands for the energy of bandgap.

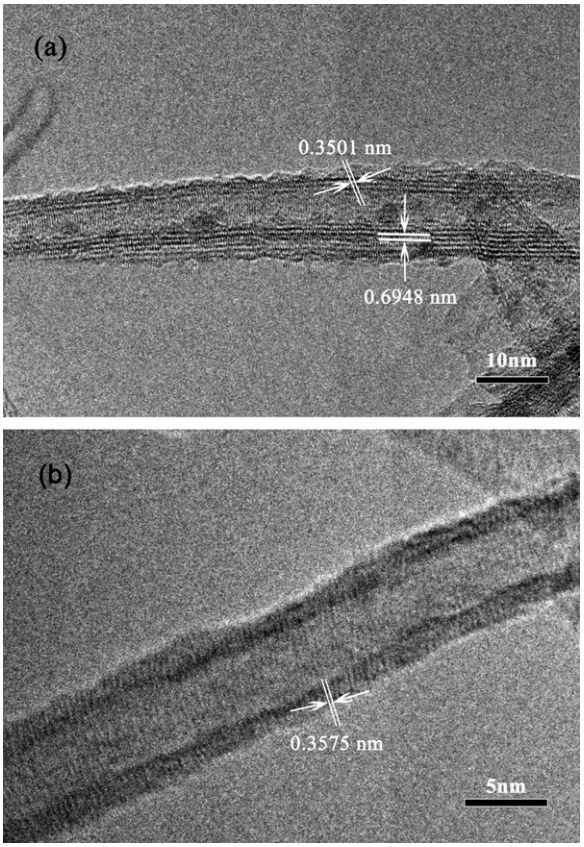

Fig. 8. The high resolution TEM images of titanium based nanotubes. (a) TNT(Na) and (b) TNT(H).

plots of the square root of $F(R)h\upsilon$ versus photon energy (as shown in Eq. (2)). Here, $h\upsilon$ is the photon energy, and E_g is bandgap energy of the semiconductor. Fig. 7 shows the estimated bandgaps of all these materials:

$$\sqrt{F(R)h\upsilon} = c(h\upsilon - E_g) \quad (2)$$

The energy bandgap of titanium based nanotubes is 3.70 eV estimated from the tangent line in the plot of the square root of Kubelka–Munk functions $F(R)h\upsilon$ against photon energy $h\upsilon$, as shown in Fig. 7a. It was observed that the bandgap of TNT(H) is smaller than that of TNT(Na) because of the ions exchange between sodium ions and hydrogen ions. The bandgaps of lead ion-exchanged TNN and TNA (Fig. 7c and e) are 3.30 eV and 3.12 eV lower than that of its precursor TNT(Na). However the bandgaps of THN and THA (Fig. 7d and f) are almost the same as THT(H). Since XRD analysis indicated that THT(H) has poor ion exchangeability, it is not surprising that the bandgaps of THN and THA did not change much as compared to that of its precursor THT(H).

3.3. Mechanism of ion-exchange reaction

So far, both XRD and bandgap analysis results indicate that TNT(Na) can be ion-exchanged by Pb^{2+} ions, but TNT(H) cannot. To investigate the mechanism of the ion-exchange process, HRTEM images were taken as shown in Fig. 8. From the high resolution images, layered microstructure can be obviously observed in TNT(Na) and two sets of lattice fringes are clearly indicated. Based on FFT (Fast Fourier Transform) calculation, the interplanar spacing of TNT(Na) was estimated to be ca. 0.3501 nm, corresponding to crystal plane (1 0 1) in anatase phase. The interlayer spacing of TNT(Na) was calculated to be ca. 0.6948 nm. The wall thickness of TNT(Na) is asymmetric, having three layers on one side and five layers on the other. This indicates that the nanotubes may be formed by scrolling conjoined multilayer nanosheets. The vacant space between layers provides reactive opportunity for lead ions. The results of ion-exchange experiments demonstrate that lead ions can be ion-exchanged with TNT(Na) freely. The reaction between TNT(Na) and different lead ions containing solution is shown as in Eq. (3):

$$Na_2Ti_3O_7 \text{ nanotube} + Pb^{2+} \rightarrow PbTi_3O_7 \text{ nanotube} + 2Na^+ \quad (3)$$

Meanwhile, we examined the microstructure of TNT(H). The fine fringe perpendicular to TNT(H) nanotube orientation is estimated to be ca. 0.3575 nm. However, the protonated TNT(H) does not show the lamellar structure, which is probably due to the important role of sodium ions in supporting layer structure. In other words, when the smaller ions H^+ (ionic radius 0.0012 nm) replace the Na^+ ions (ionic radius 0.102 nm) and fill in the interval of two layers, the layers collapse down. Therefore, the precursor TNT(H) does not possess ion exchangeability, because the non-layered structure of TNT(H) nanotubes inhibits the ion-exchange reaction between hydrogen ions and lead ions.

In addition, the ionic radius of Pb^{2+} ion is about 0.119 nm, similar to that of sodium ion. Therefore, according to the space effect of layers in nanotubes, TNT(Na) can be ion-exchanged with Pb^{2+}, while TNT(H) cannot. It has been proved by XRD patterns and bandgap analysis. The bandgap of THA and THN which is similar to the precursor TNT(H)'s bandgap indicates that there is no ion-exchange reaction between Pb^{2+} and $H_2Ti_3O_7$ nanotubes.

It is noteworthy that although TNT(H) does not posses ion exchangeability with Pb^{2+} ions, it is possible that Pb^{2+} ions can be adsorbed on the surface of TNT(H). According zeta potential analysis TNT(H) in aqueous media are known to develop a zeta potential, which is measured negative (ca. -31.06 ± 4.27 mV). However, zeta potential of TNT(Na) is around zero (ca. -0.08 ± 2.96 mV). Both pH values of measured suspension are 7.0. Therefore, although H^+ cannot be exchanged by Pb^{2+} ions, the Pb^{2+} cations can be adsorbed onto the $H_2Ti_3O_7$ nanotubes surface based on the electrostatic interactions between nanotubes suspended in aqueous solution and lead ions. Some literatures [36,47,48] have demonstrated the protonated titanate nanotubes can carry stronger negative surface charges and thus offer electrostatic binding sites for cations. This behavior of protonated titanate nanotubes dissociation can be expressed by Eq. (4):

$$H_2Ti_3O_7 \leftrightarrow H^+ + HTi_3O_7^- \quad (4)$$

Therefore, a small amount of Pb^{2+} ions can be adsorbed onto the surface of protonated titanate nanotubes. The surface adsorbed Pb^{2+} ions cannot be detected by XRD and does not change the range of light absorption either.

4. Conclusions

One dimensional titanium based nanotubes TNT(Na) and TNT(H) were prepared by the hydrothermal method, and then lead titanate nanotubes were synthesized by ion-exchange reaction between Pb^{2+} ions and Na+ ions. However, no effective ion-exchange reaction happens between Pb^{2+} ions and H^+ ions in TNT(H). This distinct difference can be explained by the layer space effect in nanotubes, namely, the interlayer of TNT(Na) provides enough space for ion-exchange reaction between sodium ions and lead ions, while the non-layered structure of TNT(H) prohibits the reaction. For the first time, we distinguished the difference in ion exchangeability between sodium titanate nanotubes and protonated titanate nanotubes. The DRS analysis of the samples reveals that the exchanged lead ions effectively narrow the bandgap of the nanotubes. However, Pb^{2+} ions adsorbed on the surface of titanate nanotubes do not change their bandgap.

Acknowledgments

We gratefully acknowledge financial support from Program for New Century Excellent Talents in University (NCET-08-0511) and National Science Foundation of China (NSFC 50672089).

References

[1] S. Sreekantan, L.C. Wei, J. Alloys Compd. 490 (2010) 436–442.
[2] Y. Wu, J. Yu, H.M. Liu, B.Q. Xu, J. Nanosci. Nanotechnol. 10 (2010) 6707–6719.
[3] M.W. Xiao, L.S. Wang, X.J. Huang, Y.D. Wu, Z. Dang, J. Alloys Compd. 470 (2009) 486–491.
[4] M.Y. Guo, M.K. Fung, F. Fang, X.Y. Chen, A.M.C. Ng, A.B. Djurisic, W.K. Chan, J. Alloys Compd. 509 (2011) 1328–1332.
[5] R.A. Doong, I.L. Kao, Recent Pat. Nanotechnol. 2 (2008) 84–102.
[6] H. Zhang, X.P. Gao, G.R. Li, T.Y. Yan, H.Y. Zhu, Electrochim. Acta 53 (2008) 7061–7068.
[7] C.M. Rodrigues, O.P. Ferreira, O.L. Alves, J. Brazil Chem. Soc. 21 (2010) 1341–1348.
[8] C.K. Lee, H.C. Chen, S.S. Liu, F.C. Huang, J. Taiwan Inst. Chem. E 41 (2010) 373–380.
[9] L. Xiong, W. Sun, Y. Yang, C. Chen, J. Ni, J. Colloid Interface Sci. 356 (2011) 211–216.
[10] N. Wang, H. He, X. Li, L. Han, C. Zhang, J. Alloys Compd. 506 (2010) 293–296.
[11] Z.W. Tang, L.Q. Zhou, L. Yang, F. Wang, J. Alloys Compd. 481 (2009) 704–709.
[12] A. Riss, T. Berger, H. Grothe, J. Bernardi, O. Diwald, E. Knozinger, Nano Lett. 7 (2007) 433–438.
[13] T. Kasuga, M. Hiramatsu, A. Hoson, T. Sekino, K. Niihara, Langmuir 14 (1998) 3160–3163.
[14] S.J. Kim, Y.U. Yun, H.J. Oh, S.H. Hong, C.A. Roberts, K. Routray, I.E. Wachs, J. Phys. Chem. Lett. 1 (2010) 130–135.
[15] N. Wang, H. Lin, J.B. Li, X.Z. Yang, B. Chi, C.F. Lin, J. Alloys Compd. 424 (2006) 311–314.
[16] L. Song, L. Cao, G. Su, W. Liu, H. Liu, L. Zhu, Adv. Mater. Res. 79–82 (2009) 581–584.
[17] G. Liu, G. Li, X. Qiu, L. Li, J. Alloys Compd. 481 (2009) 492–497.
[18] J.J. Yang, Z.S. Jin, X.D. Wang, W. Li, J.W. Zhang, S.L. Zhang, X.Y. Guo, Z.J. Zhang, Dalton Trans. 20 (2003) 3898–3901.
[19] M. Qamar, C.R. Yoon, H.J. Oh, N.H. Lee, K. Park, D.H. Kim, K.S. Lee, W.J. Lee, S.J. Kim, Catal. Today 131 (2008) 3–14.
[20] L.Z. Zhang, H. Lin, N. Wang, C.F. Lin, J.B. Li, J. Alloys Compd. 431 (2007) 230–235.
[21] A. Nakahira, T. Kubo, C. Numako, Inorg. Chem. 49 (2010) 5845–5852.
[22] J.M. Cho, M.H. Sun, T.H. Kim, S.J. Cho, J. Nanosci. Nanotechnol. 10 (2010) 3336–3340.
[23] S. Chatterjee, S. Bhattacharyya, D. Khushalani, P. Ayyub, Cryst. Growth Des. 10 (2010) 1215–1220.
[24] H. Zhang, P. Liu, H. Wang, H. Yu, S. Zhang, H. Zhu, F. Peng, H. Zhao, Langmuir 26 (2010) 1574–1578.
[25] X.M. Sun, Y.D. Li, Chem. Eur. J. 9 (2003) 2229–2238.
[26] Y. Inoue, M. Uota, T. Torikai, T. Watari, I. Noda, T. Hotokebuchi, M. Yada, J. Biomed. Mater. Res. A 92 (2010) 1171–1180.
[27] M. Qamar, S.J. Kim, A.K. Ganguli, Nanotechnol. 20 (2009) 455703.
[28] N.C. Jeong, Y.J. Lee, J.H. Park, H. Lim, C.H. Shin, H. Cheong, K.B. Yoon, J. Am. Chem. Soc. 131 (2009) 13080–13092.
[29] A.J. Du, D.D. Sun, J.O. Leckie, J. Hazard. Mater. 187 (2011) 401–406.
[30] E. Erdem, A. Matthes, R. Bottcher, H.J. Glasel, E. Hartmann, J. Nanosci. Nanotechnol. 8 (2008) 702–716.
[31] J.M. Macak, C. Zollfrank, B.J. Rodriguez, H. Tsuchiya, M. Alexe, P. Greil, P. Schmuki, Adv. Mater. 21 (2009) 3121–3125.
[32] Q. Ye, L. Qiao, J. Gan, H. Cai, R. Qu, Opt. Lett. 35 (2010) 4187–4189.
[33] J.W. Bennett, I. Grinberg, A.M. Rappe, J. Am. Chem. Soc. 130 (2008) 17409–17412.
[34] H.G. Kim, O.S. Becker, J.S. Jang, S.M. Ji, P.H. Borse, J.S. Lee, J. Solid State Chem. 179 (2006) 1214–1218.
[35] H. Irie, Y. Maruyama, K. Hashimoto, J. Phys. Chem. C 111 (2007) 1847–1852.
[36] C.K. Lee, K.S. Lin, C.F. Wu, M.D. Lyu, C.C. Lo, J. Hazard. Mater. 150 (2008) 494–503.
[37] Y.Y. Zhang, W.Y. Fu, H.B. Yang, M.H. Li, Y.X. Li, W.Y. Zhao, P. Sun, M.X. Yuan, D. Ma, B.B. Liu, G.T. Zou, Sens. Actuators B: Chem. 135 (2008) 317–321.
[38] O.P. Ferreira, A.G. Souza, J. Mendes, O.L. Alves, J. Brazil Chem. Soc. 17 (2006) 393–402.
[39] Y. Guo, N.H. Lee, H.J. Oh, C.R. Yoon, K.S. Park, H.G. Lee, K.S. Lee, S.J. Kim, Nanotechnology 18 (2007) 295608.
[40] M.D. Wei, Y. Konishi, H.S. Zhou, H. Sugihara, H. Arakawa, Solid State Commun. 133 (2005) 493–497.
[41] K.P. Yu, W.Y. Yu, M.C. Ku, Y.C. Liou, S.H. Chien, Appl. Catal. B: Environ. 84 (2008) 112–118.
[42] X.S. He, C.G. Hu, H. Liu, G.J. Du, Y. Xi, Y.F. Jiang, Sens. Actuators B: Chem. 144 (2010) 289–294.
[43] B.M. Wen, C.Y. Liu, Y. Liu, Z.Y. Zhang, J. Nanosci. Nanotechnol. 4 (2004) 1062–1066.
[44] T. Torimoto, N. Nakamura, S. Ikeda, B. Ohtani, Phys. Chem. Chem. Phys. 4 (2002) 5910–5914.
[45] C. Anderson, A.J. Bard, J. Phys. Chem. B 101 (1997) 2611–2616.
[46] Y.I. Kim, S.J. Atherton, E.S. Brigham, T.E. Mallouk, J. Phys. Chem. 97 (1993) 11802–11810.
[47] D.V. Bavykin, K.E. Redmond, B.P. Nias, A.N. Kulak, F.C. Walsh, Aust. J. Chem. 63 (2010) 270–275.
[48] H. Dai, H. Xu, X. Wu, Y. Lin, M. Wei, G. Chen, Talanta 81 (2010) 1461–1466.